CONF-960757--1 ANL/TD/CP--90217

Performance of Ceramic Membrane Filters

Rajesh K. Ahluwalia (walia@td.anl.gov; 708-252-5979)
Kwan H. Im (im@td.anl.gov; 708-252-5985)
Howard K. Geyer (geyer@td.anl.gov; 708-252-5995)
Argonne National Laboratory
9700 South Cass Avenue, Building 207
Argonne, IL 60439-4841

David L. Shelleman (814-865-0634)
Richard E. Tressler (814-865-7961)
The Pennsylvania State University
101 Steidle Building
University Park, PA 16802

Introduction

CeraMem Corporation's ceramic-membrane coated, dead-end ceramic filters offer a promising alternative to ceramic candle filters provided long-term operational and reliability issues are resolved. One outstanding operational issue pertains to regenerability of filter passages by the simple back pulse technique in a repeatable manner over a time span of thousands of hours. For commercial acceptance, the tolerance of the CeraMem cordierite material to exposure to alkali-containing combustion gas, being able to absorb Na_2O without serious degradation of the mechanical properties at use temperatures, must be demonstrated. The performance must be correlated to the phase composition and microstructure after exposure.

The thermal and chemical aging at use temperature may significantly alter the thermophysical and mechanical properties of these materials in ways which must be documented. In fact, the values of thermal expansion coefficient, thermal conductivity, and elastic moduli as a function of temperature must be measured for the as-fired or as-received materials in addition to the thermally and chemically aged materials. These parameters determine the thermal gradients in the components during transient and steady state operating conditions, and the thermoelastic stresses which develop in the components as a result of these thermal gradients. The thermoelastic stresses can be accurately mapped in a given component if the temperature distributions are known (assumed and/or calculated) and the thermomechanical properties are known as a function of temperature and aging history. In conjunction with a knowledge of the strength distribution of the material as a function of temperature and aging exposure, these thermoelastic stress calculations can be used to predict survival of the components in actual or simulated use.

Research sponsored by the U.S. Department of Energy's Morgantown Energy Technology Center, FTPA Number ANL-49966, B&R Code AC-15.

DISCLAIMER

In addition, when the details of the microstructural changes are established as a function of temperature and thermochemical aging and the properties are related in a cause-effect relationship, the microstructure (phase composition, grain size, pore size and shape) can be tailored to resist the deleterious changes.

Objectives

1. Develop a fluid mechanics and particle transport model for analyzing filtration and back pulse cleaning of dead-end ceramic membrane filters.

2. Develop a data base on the effects of thermal and chemical aging on flow behavior and thermophysical and mechanical properties of ceramic filters.

3. Develop the capability of predicting the probability of survival of commercial filters under anticipated service conditions from calculated thermoelastic stresses and measured material properties.

Approach

This program utilizes combined experience, skills and facilities at three organizations: Argonne National Laboratory (ANL), Penn State University (PSU) under subcontract to ANL, and CeraMem Corp. (not funded under this initiative). ANL is responsible for analytical modeling of filtration and pulse-cleaning operations, flow-through testing, and prediction of filter response to thermal cycling under realistic service conditions. PSU is responsible for measuring properties and microstructural changes of exposed filter specimens. CeraMem is charged with the responsibility of fabricating and supplying the filters, advising ANL on its experience with pulse cleaning, and conducting exploratory or confirmatory laboratory tests as needed.

Project Description

We previously reported on the analysis of forward and reverse flows in dead-end filters, based on models for jet entrainment and mixing, fluid flow in filter passages, and venturi nozzle and diffuser [Ahluwalia and Geyer, 1996]. A test apparatus, shown schematically in Fig. 1, was assembled to expose ceramic filter specimens to chemical environments simulating operation of pressurized fluidized bed (PFB) and integrated gasification combined cycle (IGCC) plants [Ahluwalia et al, 1995]. An air-blast elutriator was fabricated to feed ash at 0.5-2 g/h. It is particularly suitable for low feed rates and highly agglomerating ash such as the ash from Tidd plant. The feed rate in this device is controlled by the transport gas throughput and the speed of the chain conveying ash from the hopper to the suspension chamber. An ultrasonic nebulizer is used to feed alkaline water containing dissolved sodium chloride or sodium hydroxide. The gas-phase alkali concentration is controlled by the alkali content of water solution, vibration frequency of the nebulizer diaphragm and the flow rate of purge gas used to entrain the mist produced by the ultrasonic action. A concentric tube arrangement is

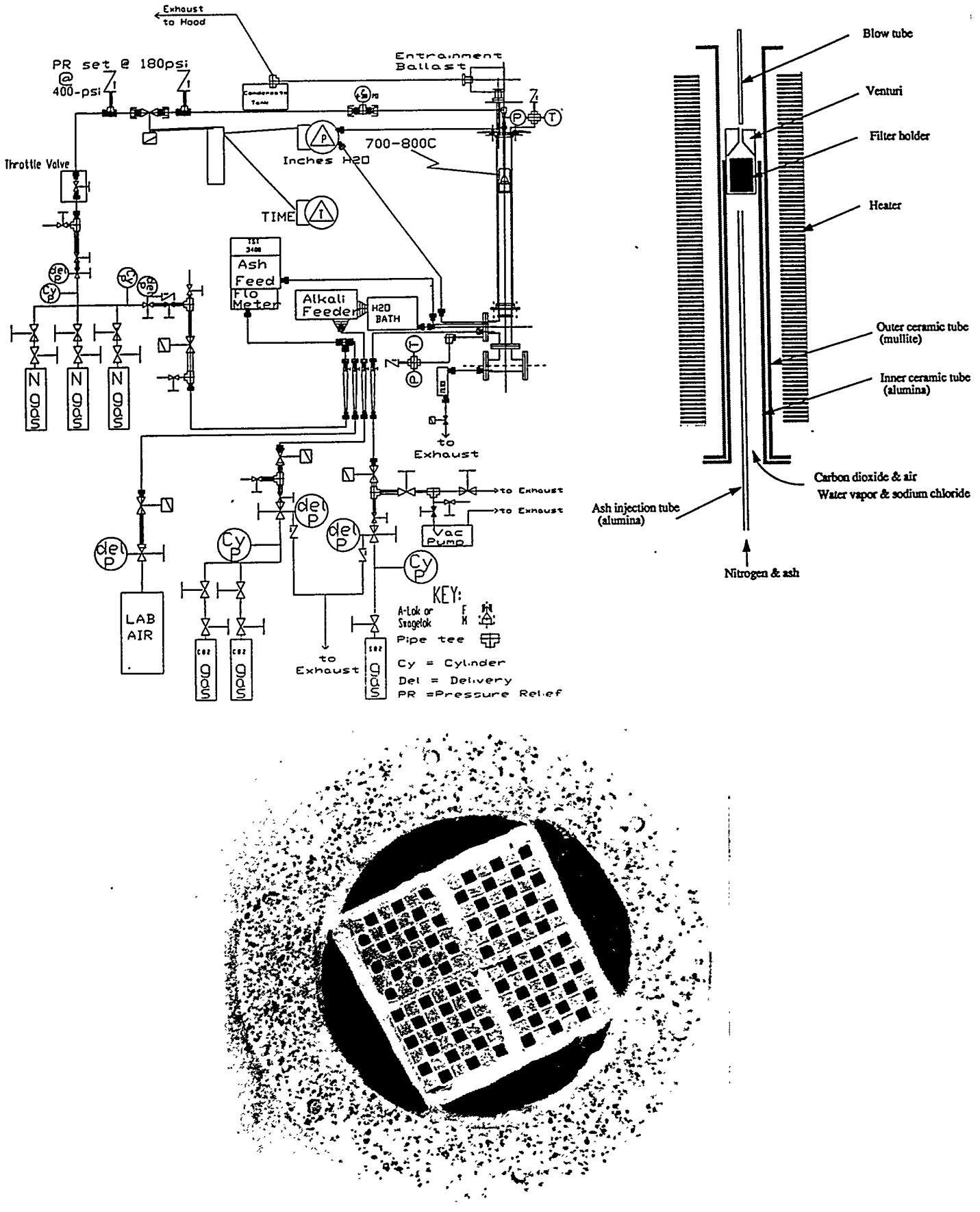

Figure 1. Schematics of the filter exposure apparatus, concentric tube arrangement and filter holder.

employed to contain and heat the gases and position the filter holder which is machined from Inconel 625 and alonized for added corrosion resistance. The holder accommodates four 6 cell x 6 cell specimens (100 cells per square inch, 5.08-cm long) surrounded by dense ceramic fillers and held together with a steel clamp. For leak-tightedness, a compressible ceramic mat is placed between the filters and between the filters and the fillers. The clearance between the filters and the filter holder is also packed with the ceramic mat.

The pulse gas from a high-pressure nitrogen reservoir is directed into a blow pipe and issues from a small blow hole of 1.25-mm diameter. It discharges into the plenum region and entrains some of the clean hot gas. The resulting mixed jet enters the venturi atop the filter holder. It is estimated that a differential pressure of about 22 kPa can be generated in the venturi at a reservoir pressure of 10 bar and a trigger pressure of 40-cm H_2O. Pulse duration and frequency are adjustable by means of a computer-controlled solenoid valve.

A number of tests were conducted to ensure leak tightness and optimize the method of assembling the filter specimens inside the holder. Extensive data was obtained to characterize the flow behavior of the clean filter. Figure 2 summarizes the selected data on filtration pressure drop (ΔP) vs flow rate at different gas temperatures and on ΔP vs temperature at different flow rates. The available data is consistent with an effective permeability of 5.9×10^{-10} m for the Ex-80 membrane-coated cordierite monolith having 48% porosity, 0.4 cc/g pore volume and 12.5 μm mean pore size.

Results

Four long-duration tests have been conducted in which 100-cpsi channel filters were exposed to ash collected downstream of the cyclone separator at the PFBC plant at Tidd. The median diameter of ash is 2.8 μm and the top size is less than 10 μm. The pressure drop across the filters was monitored during the test. A data base has been established on the microstructure and the mechanical properties of the as-received filter material. Effect of thermal aging on the mechanical properties has been determined. Measurements are continuing to determine the changes in the microstructure and the mechanical properties after exposure in the four tests.

System Checkout. A long duration test (Run 1) lasting twenty-five days, was run to study the behavior of system components under different operating conditions. The apparatus was operated in an attended mode in which ash and alkali were fed during the day time only. There was no SO_2 injection and the pulse valve was operated manually. Figure 3 shows the pressure trace for different gas temperatures (800-950°C furnace temperature), gas flow rates (6.4-10 slm), pulse gas reservoir pressures (7.8-11.2 bars), time between pulses (0.5-5 h), and number of pulses (1-4). The tests confirmed the existence of a conditioning time during which the baseline filtration pressure drop (ΔP after pulsing) increased steadily. Over the limited time span, the filters could be regenerated at 900°C by using pulse gas at 11.2 bar reservoir pressure.

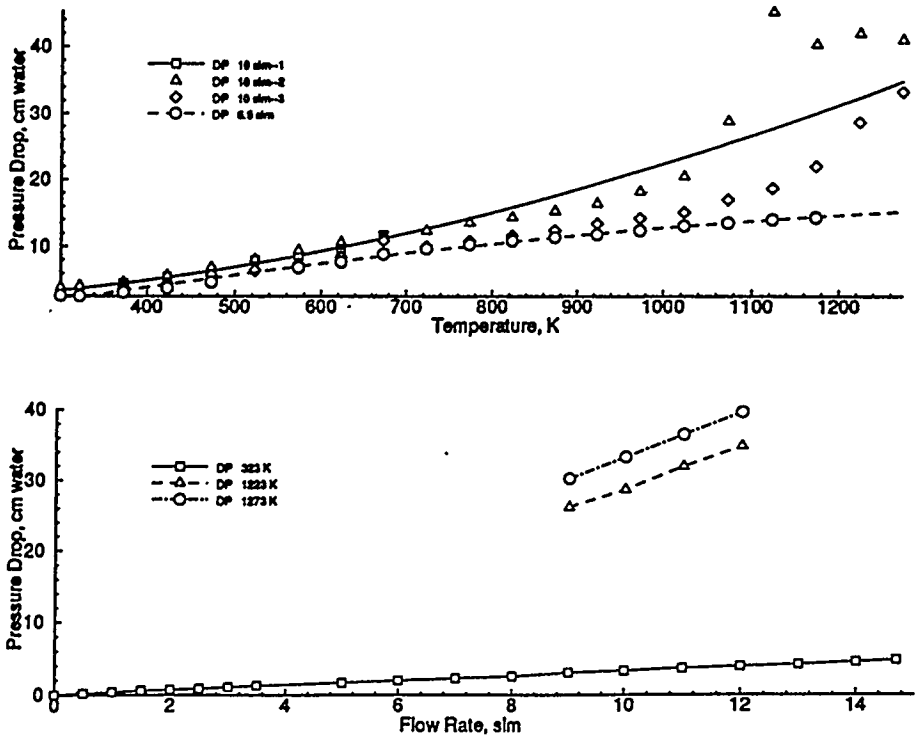

Figure 2. Pressure drop behavior of clean filter.

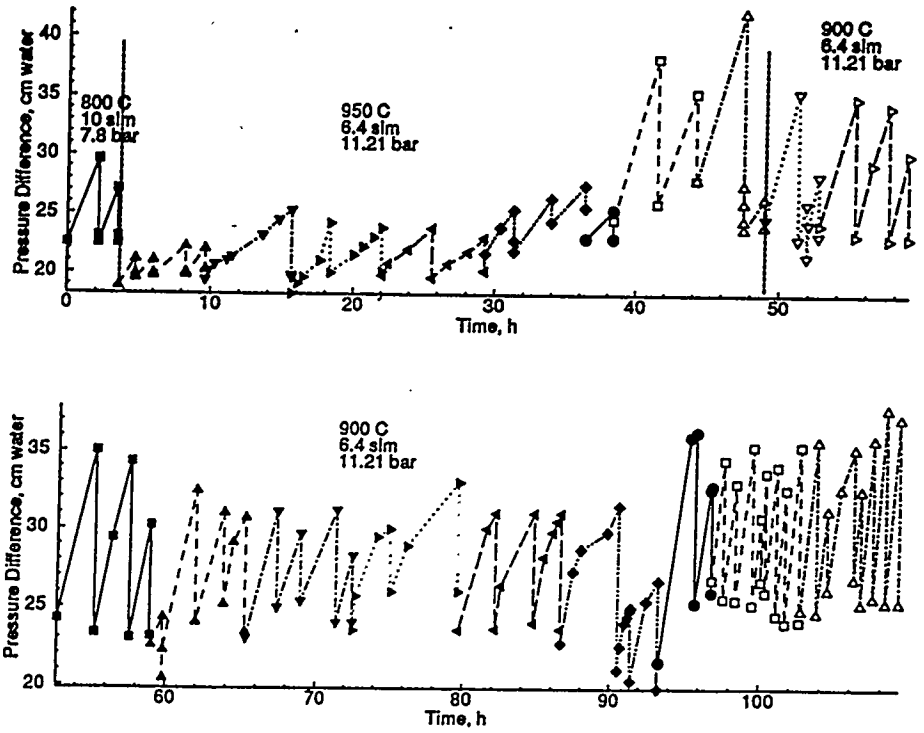

Figure 3. Filtration pressure drop and back pulse cleaning during system checkout (Run 1).

Filter regenerability was not affected by time interval between pulses. A single pulse was generally sufficient to recover to the baseline ΔP. Incremental recovery in ΔP with multiple pulses was small. Various subsystems for gas handling, gas heating, pulse gas, filtration and ash feed operated reliably although leakage problems were experienced with the alkali feed system and corrected. Post test inspection of the filter specimens revealed no visual deterioration in integrity or ash penetration across the membrane walls.

Performance at 900°C. A long duration test (Run 2) was conducted to expose filter specimens at 900°C furnace temperature. Mean gas composition was 75.2% N_2, 13.9% CO_2, 3.3% O_2 and 7.6% H_2O. The contaminant loading was 900 ppmw ash, 70 ppmv alkali and 250 ppmv SO_2. The operation of the solenoid valve was computer controlled. A single pulse of nominal 1 s duration was used. The pulse frequency was 3/h at start of the test (0-18 h), once every hour during much of the test (18-1008 h), and increased to 2/h near the end. The reservoir gas pressure was 7.8 bar at start of the test (0-268 h), raised to and maintained at 9.8-11.3 bar during the middle portion (268-1015 h), and raised further to 14.6 bar near the end. Figure 4 depicts the pressure drop behavior at 2.4 cm/s face velocity. The data indicates a filter conditioning time of about 100 h during which the baseline ΔP increased from 15-cm H_2O (clean filter ΔP) to about 30-cm H_2O. Between 200-900 h, a steady saw-tooth ΔP profile was established with a pressure swing of about 7-10 cm H_2O between the pulses. Some ΔP excursions were observed due to an unresolved bug in the control software which unpredictably missed 1-5 pulse cycles at a time. Some excursions were caused by the heated line between the nebulizer and the inlet plenum developing a blockage due to NaCl deposits. In the steady-state mode of operation, the system was able to recover from these excursions. At about 980 h, both baseline ΔP and the pressure swing between the pulses started to climb gradually. At 1008 h, the pulse frequency was doubled after the pressure swing had reached 20-cm H_2O. This had the favorable effect of controlling the pressure swing although the baseline ΔP continued to climb slowly. At 1015 h, the reservoir pressure was raised to 14.6 bar in an attempt to control the baseline ΔP. Although temporarily successful, baseline ΔP resumed its climb. The situation was exasperated by the control software missing three consecutive pulses. At this point, the filter specimens could not be regenerated resulting in termination of the test.

Figure 4 also presents the fine details of pressure recovery following a pulse operation. It shows ability to regenerate the filter passages after pressure excursions as at 50 h, 385 h and 1000 h. It indicates limited incremental benefit in going to double (225 h, 275 h and 315 h) and triple (275 h and 1000 h) pulses spaced 200 to 400 s apart. For the filter specimens used in these tests, the characteristic time for pressure recovery appears to be less than 50 s.

Post test inspection revealed that the ceramic ash transport tube was clean. There were mounds of ash built up on the cement plugs at filter inlet. All channels were accessible to gas flow. There was no visual evidence of ash penetration across to the

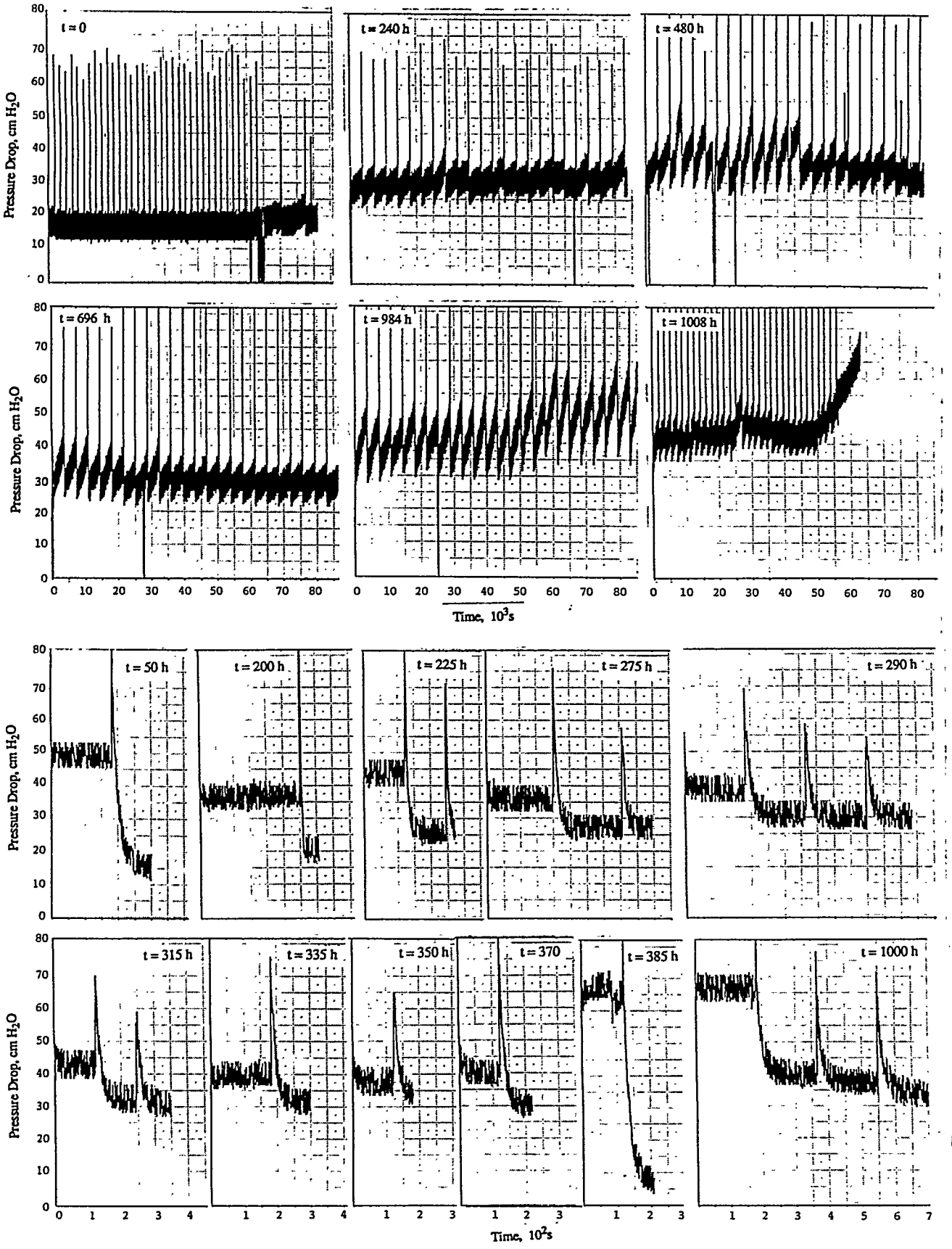

Figure 4. Pressure traces from 1050-h test at 900°C (Run 2).

clean channels or of ash sintering. There were metal corrosion products on top of the venturi which came from the ballast tank. There was minimal deterioration of the alonized filter holder and venturi but the metal screws joining the holder and venturi were severely corroded and easily broken (as designed). Ash at various locations had different coloration. In order to analyze the pattern of residual ash filling up the passages, the channels were probed with a thin wire. From the resistance felt while inserting the wire, it was concluded that there was considerable variation of the residual ash content in the channels and along the passage length. To confirm these observations, one of the filter specimens was cracked near mid length. Optical macrographs of the fractured filter surface indicate that the channels are severely filled with ash.

Three of the four exposed filter specimens contained several transverse cracks which were clearly visible on the outer surfaces. The cracks are believed to have been caused by overtightening of the steel clamp used to hold the filter specimens together.

As stated earlier, several operational problems were encountered in Run 2 due primarily to the control software skipping several pulse cycles. This resulted in overpressurization of the inlet plenum and flow leakage from the glass tank housing the nebulizer. The leakage problem was solved with a redesign leading to the elimination of the glass tank. In order to resolve the effect of pressure excursions on the observed flow behavior, it was decided to repeat the test (Run 3) with a new control software employing a pulse schedule closer to the field practice. The schedule consisted of a double pulse, each of 100-ms duration and 100-ms apart. To minimize possible ash-membrane interaction, the pulse frequency was changed to 3/h regardless of ΔP. The test ran smoothly without experiencing any problems with ash feed, alkali injection or pulse gas system. The system was shut down for Christmas break after 364-h. Upon restart, the filters could not be regenerated with back pulsing and the test was terminated after 388-h exposure. The post test observations revealed no visual signs of filter deterioration. There were no surface transverse cracks since care was taken to not overtighten the steel clamp. Much later during Run 4, it was realized that the failure to regenerate the filter was related to the nozzle (blow hole) being nearly blocked by a small quantity of metal corrosion products. The blockage was easily relieved with water washing.

Performance at 800°C. A 2000-h test (Run 4) was conducted in which the filter specimens were exposed to simulated combustion gas (3.3% excess oxygen) containing 7.6% H_2O, 11.2 ppmv NaCl and 1011 ppmw entrained ash. The filters were maintained at 800°C. A single pulse of 1-s duration was used to regenerate the filter passages. Initially, the time interval between the pulses was set at 30 min which was reduced to 15-20 min as the ΔP swing became larger. Right at the start of the test, difficulty was experienced in regenerating the filter passages and was traced to the blow hole being blocked by the blow-tube corrosion products. The blockage problem was alleviated by continuously purging the blow tube with a small quantity of N_2 (less than 0.5 slm) and isolating it from the alkali rich gas. The reservoir pressure for pulse

gas varied between 11.2 and 14.6 bars. As indicated in Fig. 5, the baseline ΔP was stable at 30-32 cm H_2O for exposure time less than about 1000 h. Over a longer time period, it gradually crept up to above 50-cm H_2O. Consistent with the earlier experience, ΔP swing increased with exposure time from 1-cm H_2O to 10-cm H_2O. At various times attempts were made to investigate if the residual ash could be dislodged by allowing the filters to cool down to a lower temperature, back pulsing and raising the temperature back to 800°C. The results were not encouraging although some success was gained early in the test. The observed variation of ΔP with temperature was quite remarkable (Fig. 6). For a clean filter, a single value of effective permeability (K_{eff}) can explain the measured ΔP as a function of temperature and flow rate. An exposed filter, after cold pulsing, has K_{eff} which is a strong function of temperature. After 1000-2000 h exposure, K_{eff} has even stronger temperature dependence.

Strength. Table I summarizes the average strength and standard deviation of the flexure specimens machined from as-received, thermally aged, and exposed filters. No significant changes in strength were observed as a function of temperature or membrane coating for the as-received 25 cpsi filters. Even after thermal aging at 800°C for 1000 hours, only a slight increase in strength was observed at 870°C.

Flexure specimens machined from filters exposed at 1600°F for 300 hours at the Ahlstrom Pyropower combustor in San Diego exhibited no significant changes in strength with the possible exception of the 870°C data which showed a slight strength increase (depending on lot-to-lot variations).

As for the 100 cpsi filters, strengths that were independent of test temperature were again observed at 800°C and 870°C. However, flexure specimens from filters exposed in Runs 3 and 4 exhibited approximately 44% and 33% reductions in strength, respectively. Even with the limited number of specimens tested (5 for Run 3 and 7 for Run 4) a relatively large amount of scatter was observed in the strength measurements, which suggests that hot corrosion of these filters may not be uniform. Additional strength testing and detailed characterization are needed to quantify the effects of hot corrosion on these filters.

The observed reductions in strength may be associated with the alkaline content used in the exposure runs. Flexure specimens from filters exposed in Run 3 exhibited a 44% reduction in strength and were exposed to ~70 ppm of sodium, while flexure specimens from filters used in Run 4 exhibited a 33% reduction in strength and were exposed to ~11 ppm of sodium. Powders from filters used in Runs 3 and 4 were analyzed by x-ray diffraction. While definite peaks for the nepheline [(Na, K) Al SiO_4] are present in the pattern obtained from filters exposed in Run 3, nepheline peaks are not as evident in the pattern for filters from Run 4. Peaks corresponding to nepheline may be present in pattern from Run 4 but are on the order of the background noise level.

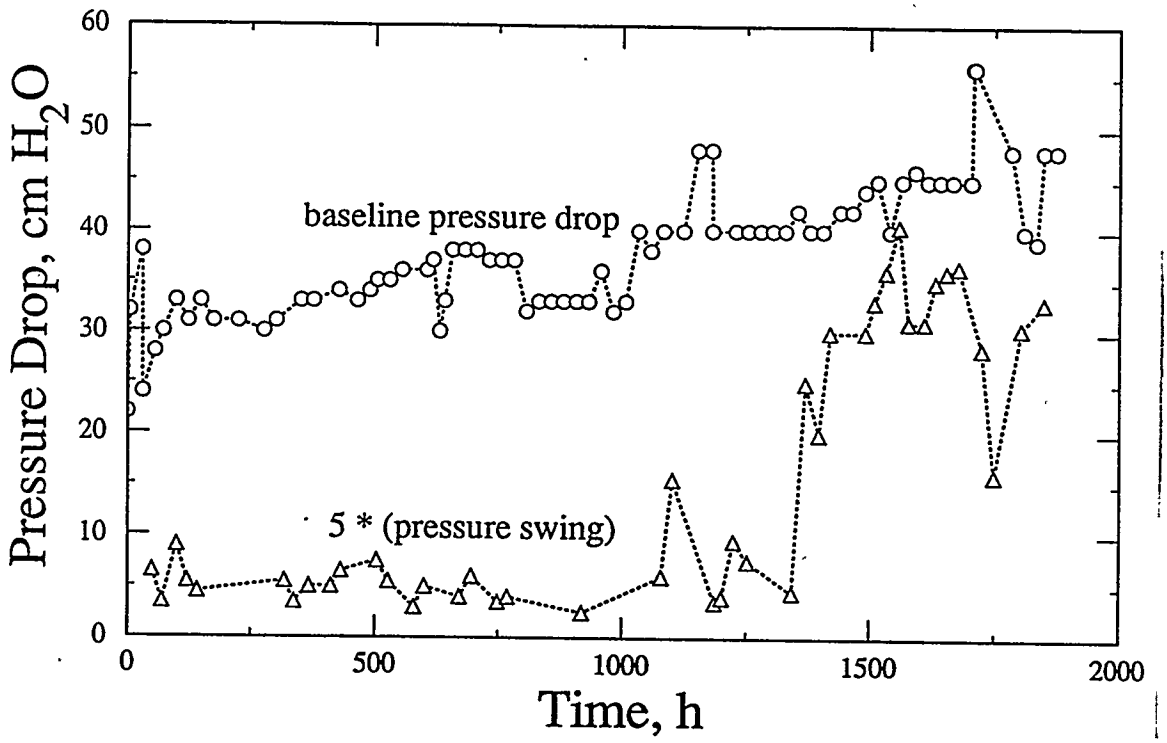

Figure 5. Variation of baseline pressure drop and pressure swing during the 2000-h test at 800°C (Run 4).

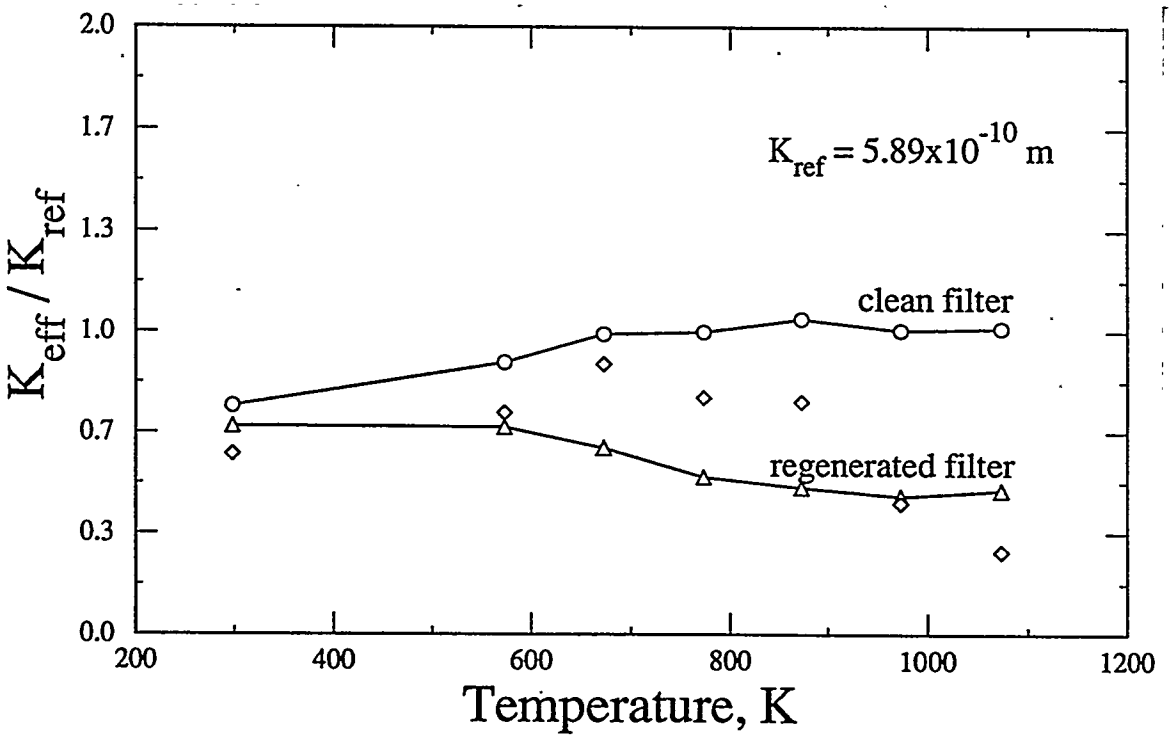

Figure 6. Temperature dependence of filtration pressure drop for clean (o) and regenerated (Δ, ◇) filters.

Table I. MOR (Modulus of Rupture) strength data from four-point bend tests

Size	Condition	Strength, MPa		
		25°C	800°C	870°C
25 cpsi	As-received, Uncoated	9.5±0.6	9.7±1.5	10.8±1.3
	As-received, Coated	10.1±0.4	10.2±1.3	10.4±0.9
	As-received, Coated 1000 hrs @ 800°C	9.1±0.8	11.4±0.9	11.0±0.8
	Ahlstrom 300 h[a]	10.4±0.7	12.3±2.2	12.5±1.0
	Ahlstrom 300 h[b]	10.9±0.7	11.3±1.8	10.7±1.5
100 cpsi	As-received, Coated	8.8±0.8	8.4±0.9	8.6±1.5
	Run 3: 388 h @ 900°C		4.7±2.0	
	Run 4: 2000 h @ 800°C		6.5±2.6	

a - Tensile surface of flexure specimen was from clean side of filter channel.
b - Tensile surface of flexure specimen was from filtering side of filter channel.

The reaction of cordierite with alkalis (Na and K) to form nepheline may be a possible hot corrosion mechanism that could lead to a reduction in the strength of these filters. Nepheline has a thermal expansion coefficient that is at least 10 times greater that of cordierite. Such thermal expansion difference could lead to the formation of microcracks which can weaken the filters. The formation of microcracks will decrease the elastic modulus of the material (as discussed in the following section). Due to the size and geometry of the 100 cpsi filters, we were not able to measure the elastic modulus of the exposed filters to determine if the modulus of the exposed filters is significantly lower than that of the unexposed filters. Exposure testing of the 25 cpsi filters would enable us to measure the elastic modulus of the exposed filters. Additional strength testing and characterization are needed to verify that nepheline is the source of the strength degradation in these exposed filters.

Elastic Modulus. The elastic modulus of the 25 cpsi filters were measured as a function of temperature using the acoustic resonance technique. Samples six cells wide by two cells thick by two inches in length were machined from the as-received uncoated, coated, and exposed filters from Ahlstrom Pyropower to measure the structural stiffness (E_s) of the filters as a function of temperature (both heating to 950°C and cooling to room temperature). The structural stiffness of the filters was then multiplied by the ratio of the cell length to the thickness of the cell walls (l_s/w_s) to calculate the elastic modulus (E^*) of the material.

Table II. Elastic modulus data for 25-cpsi filter specimens

	Structural Stiffness, E_S (GPa)				Elastic Modulus of Material, E* (GPa)			
	Uncoated	Coated	A300[1]	T1000[2]	Uncoated	Coated	A300[1]	T1000[2]
Heating (°C)								
22	2.6	2.4	2.2	2.2	13.2	9.9	10.2	9.2
400	2.7	2.5	2.4	2.3	13.3	10.1	11.0	9.4
800	3.1	3.2	2.6	3.0	15.5	13.4	12.0	12.4
870	3.3	3.4	2.7	3.2	16.6	14.4	12.5	13.2
950	3.5		2.7	3.5	17.5	12.6		14.6
Cooling (°C)								
870	3.6	3.8	2.8	3.6	17.8	15.8	13.1	14.9
800	3.6	3.7	2.9	3.6	17.9	15.5	13.5	14.9
400	3.0	2.9	2.8	2.9	15.2	11.9	12.8	11.8
22	2.6	2.4	2.2	2.2	13.2	9.9	10.6	9.1

* Based on the following equation: $E^*=E_S$ (Strut length/Strut thickness).
[1] CeraMem filters exposed for 300 h at 1600°F in a combustor at Ahlstrom Pyropower.
[2] CeraMem filters (25 cpsi) thermally aged for 1000 h at 800°C.

As was observed for the strength of these filters, the elastic modulus of the material was not significantly affected by the coating or thermal aging (see Table II). The elastic modulus does exhibit a hyteretic behavior upon heating and cooling which is presumably caused by closing and opening of microcracks. As the material is heated, microcracks that formed during cooling from processing temperature, begin to close and continue to close up to 1000°C. The closure of microcracks results in an increase in the elastic modulus of the material. Upon cooling, the microcracks begin to open around 650°C and the modulus decreases with temperature.

Microstructural Characterization. Scanning electron microscopy and energy dispersive x-ray spectroscopy were used to investigate possible ash/membrane interaction on the exposed filters. Three out of four 100 cpsi filters exposed in Run 2 (~1050 hours at ~850°C) contained transverse cracks, which resulted from excessive clamping forces used to mount the filters in the exposure rig. Filter #2, which possessed some cracks, was deliberately fractured in half across its width to analyze the microstructure of the filter walls, membrane, and ash for possible interactions. There was some evidence of necking between ash particles near the membrane suggesting that ash-membrane interactions may

have occurred. The necking of the ash particles, while not necessarily resulting in densification of the ash, does indicate that liquid phase sintering may have occurred. The particles of ash located towards the center of the filtering cell did not show evidence of necking, but resemble agglomerates of individual ash particles.

Optical microscopy was used to examine fractured flexure specimens machined from a filter used in Run 4 (2000 hours at 800°C) and tested at 800°C. The ash in one of the two filtering cells was seen to have pulled out of the opposing cell when fractured. This suggests that there was no significant bonding between the ash and the membrane coating. A higher magnification micrograph of the ash adjacent to the membrane and near the center of the cell revealed no evidence of ash/membrane interactions or necking between ash particles.

Energy dispersion spectroscopy was used to identify elements present in the ash. A series of EDS patterns were obtained starting from the cell wall on the clean side of the cell through to the ash in the center of the filtering cell. With the exception of detecting Mg, Al, and Si from the cordierite of the cell wall as well as elements associated with the proprietary membrane coating, high concentrations of calcium, iron and sulfur were detected in the regions of the ash, but the sodium level did not vary much from one region of the filter to the other.

Discussion

A bench-scale, flow-through apparatus has been assembled for continuous, unattended exposure of ceramic filter specimens to oxidizing and reducing environments of PFBC and IGCC plants. Feed systems are provided for introducing ash, alkali and sulfur impurities into the gas stream. The apparatus includes an on-line pulse gas system to dislodge the ash deposits from the ceramic filters after accumulation for a defined interval of time or to a defined pressure drop.

Four long-duration tests have been completed to characterize the filtration and pulse cleaning behavior of CeraMem's ceramic filters with 2-mm square channels. The tests were conducted under oxidizing conditions. The test data indicates a conditioning time during which the pressure drop increases to a steady-state value. A repetitive saw-tooth ΔP profile is maintained for 200-900 h at 900°C and for more than 1000 h at 800°C. Beyond this time, the baseline ΔP and the pressure swing between consecutive pulses begin to climb gradually. A stage is asymptotically approached where the filters cannot be regenerated online by the simple back pulse technique. For exposure times exceeding 1000 h, attempts to pulse-clean the filters at lower than the working temperature proved unsuccessful. It remains to show whether a fouled filter can be taken off line and regenerated with a water rinse.

For the test conditions investigated, filter cleanability is not affected by the pulse schedule, i.e., a single pulse performed as well as a multiple pulse. The filters display a remarkable ability to recover after severe ΔP excursions due to system upsets

(missed pulses). At 900°C and 70 ppmv NaCl concentration SEM micrographs exhibit some membrane-ash interaction and necking between the ash particles deposited on the membrane. No such interactions were observed at 800°C and 11 ppmv NaCl concentration when the pulse schedule was more frequent (15-30 min pulse interval vs. up to 1 h at 900°C). Post test examinations revealed that the filter passages were quite filled with residual ash. Thus, the reason for measured creep in baseline ΔP at long exposure time is not related to ash sintering to the filter membrane but is of fluid mechanic origin. The phenomenon of residual ash filling up the passages has also been observed in other tests with 4-mm channels. Based on the measured temperature dependence of ΔP, it appears inappropriate to describe the pressure drop by porous media equations when the filter passages are filled with ash.

A data base has been established on the mechanical properties of as received membrane-coated cordierite material, properties after thermal aging, and after chemical exposure. Four-point flexure tests on 4-mm cell size coated and uncoated as-received specimens exhibit only a small increase in strength with temperature in the range 20-870°C (mean strength about 10 MPa). Little change in strength was measured (±10%) after thermal aging the specimens for 1000 h in a furnace at 800°C. The measured strength decreased by more than 60%, to 4.7±2 MPa at 800°C, after the filters were exposed to contaminants (70 ppmv NaCl concentration) at 900°C for 388 h (Run 3). The strength data for the exposed filters was averaged over six test specimens. The data had a large variation, from 2.6 to 7.9 MPa. The reduction in strength was somewhat smaller (35% to 6.5±2.6 MPa at 800°C) for the filters exposed to simulated combustion gas containing 11 ppmv NaCl at 800°C for 2000 h (Run 4).

A possible hot corrosion mechanism has been identified which involves the reaction between the cordierite and alkalis to form nepheline. During pulse cleaning, the filter is subjected to thermal cycling which may produce microcracks because of the large differential in the thermal expansion coefficients for nepheline and cordierite. It is proposed that the microcracks are responsible for the observed degradation in strength.

Future Activities

The immediate focus of this project has now shifted to exposing the advanced candle filter specimens to reducing gas environments containing NaCl, H_2S, H_2O and gasification ash. The fibrosic candle (15.2 cm long, 5.6 mm outer diameter) manufactured by Industrial Filter and Pump Manufacturing Company (IFPM) will be the first to be tested. In the meantime, work is continuing on characterizing the microstructure and measuring the mechanical properties of the CeraMem filter specimens exposed in Runs 1-4. In a parallel effort, modeling work is being initiated to use the material property database being generated in this project and predict the probability of survival of commercial filters under anticipated service conditions.

References

Ahluwalia, R.K. and Geyer, H.K., "Fluid Mechanics of Membrane-Coated Ceramic Filters," To appear in ASME Journal of Engineering for Gas Turbines and Power, Vol, 118, July 1996.

Ahluwalia, R.K., Geyer, H.K. et al, "Assessment of Ceramic Membrane Filters," Proceedings of the Advanced Coal-Fired Power Systems' 95 Review Meeting, 279-291. DOE/METC-95/1018. NTIS/DE 95009732. Springfield, VA: National Technical Information Service.

Acknowledgement

This research is sponsored by DOE-METC with Dr. Norman Holcombe as the project manager. Dr. Chao Zhu of ANL assisted in assembling the apparatus and conducting Runs 1 and 2. Dr. Vince Novick is a consultant to this project. Jim Nasiatka is responsible for maintenance of the test apparatus.